ORIGINAL PAPER

Role of root hair elongation in rhizosheath aggregation and in the carbon flow into the soil

Pedro Paulo C. Teixeira[1] · Svenja Trautmann[2] · Franz Buegger[3] · Vincent J. M. N. L. Felde[4] · Johanna Pausch[5] · Carsten W. Müller[1,6] · Ingrid Kögel-Knabner[1]

Abstract

One of the most prominent changes in the rhizospheric soil structure is associated with the formation of a strongly bound soil layer in the surroundings of the root, which is named rhizosheath. In this study, we investigated how root hair elongation, a ubiquitous root morphological trait, affect the stability of rhizosheath aggregates. Using $^{13}CO_2$ pulse labeling, we tracked the fate of root-derived ^{13}C inputted into the rhizosheath of two *Zea mays* L. genotypes with contrasting root hair elongation: a mutant with root hair defective elongation (*rth3*) and a corresponding wild type (WT). In addition, we also investigated the differences between two $^{13}CO_2$ labeling approaches (single vs. multiple pulse labeling) in the distribution of ^{13}C in the rhizosheath aggregates. We were able to demonstrate that the rhizosheath aggregate stability and the resulting aggregate size distribution follows the same mechanisms irrespective of the root hair elongation. This result reinforces the assumption that other soil properties are more decisive for the soil structure formation in the rhizosheath in comparison to root hair elongation. The majority of recently deposited root-derived C (57%) was found in the macroaggregates. Increasing the number of pulses (multiple pulse labeling approach) resulted in a higher ^{13}C enrichment of the rhizosheath aggregates fractions in comparison to the application of a single pulse. While both labeling approaches resulted in a similar distribution of ^{13}C in the rhizosheath aggregates, the higher enrichment given by multiple pulse labeling allowed the separation of significant differences between the genotypes in plant C allocation in the rhizosheath.

Keywords Rhizosheath · ^{13}C pulse labeling · Isotopes · Dry-crushing · Maize (*Zea mays* L.) · Rhizosphere soil aggregates

Introduction

Soil aggregation is a key ecosystem process mediated by a wide range of abiotic and biotic factors (Six et al. 2004; Bucka et al. 2021). Among these factors, roots are recognized as major drivers for the formation and stabilization of aggregates (Tisdall and Oades 1982; Baumert et al. 2021). The capacity of roots to affect soil aggregation depends on a large number of root traits (Gould et al. 2016). Linking root traits to specific ecological processes in soils, such as aggregate formation, is still a knowledge gap in trait-based ecology research (Bardgett et al. 2014; Poirier et al. 2018; Baumert et al. 2018).

Root hairs are a ubiquitous morphological root trait formed by the protrusions of root epidermal cells (Dolan and Costa 2001; Brown et al. 2017). Despite being regarded as an important factor for plant water and nutrient acquisition (Jungk 2001), root hairs may have a yet overlooked role in soil aggregation. The presence of root hairs has often been

✉ Pedro Paulo C. Teixeira
pedro.paulo.teixeira@tum.de

1 Chair of Soil Science, TUM School of Life Sciences, Technical University of Munich (TUM), Freising-Weihenstephan, Germany

2 Department of Geography, University of Innsbruck, Innsbruck, Austria

3 Institute of Biochemical Plant Pathology, Helmholtz Zentrum München (GmbH), German Research Center for Environmental Health, Neuherberg, Germany

4 Institute of Soil Science and Soil Conservation, Justus Liebig University Giessen, Giessen, Germany

5 Department of Agroecology, Bayreuth Center of Ecology and Environmental Research (BayCEER), University of Bayreuth, Bayreuth, Germany

6 Department of Geosciences and Natural Resource Management, University of Copenhagen, Copenhagen, Denmark

associated with changes in the soil structure that leads to the formation of a root-adhering soil layer (Watt et al. 1994; McCully 1999). This root-adhering soil layer is often named rhizosheath and can be understood as a specific region of the rhizosphere (region of the soil affected by roots, see Kuzyakov and Razavi 2019) which is methodologically defined by soil-bound to the root after it is taken from the ground (Brown et al. 2017).

The role of root hairs in the formation of the rhizosheath has been associated with several factors, such as the physical entanglement of soil particles (Watt et al. 1993; De León-González et al. 2007), the enhancement of root penetration (Bengough et al. 2016), the increase in root exudation and mucilage production (Watt et al. 1993; Holz et al. 2018), and the modification in rhizosphere water content (Albalasmeh and Ghezzehei 2014; Carminati et al. 2017). Despite the enormous advances in understanding the role of root hairs in shaping soil structure, no studies evaluated how the carbon (C) flow from the roots into the soil affects the rhizosheath formation and the aggregate stability therein. Since the mechanisms of soil aggregation extensively dependent on the binding action of soil organic matter (SOM), a comprehensive view of the different processes simultaneously acting in the rhizosphere needs to track the C released from roots and conceptually include the microbial transformation processes of this rhizodeposition C into SOM acting as a gluing agent for soil aggregates (Totsche et al. 2018).

The effects of root hairs in plant performance and in the soil can be assessed through the comparison of genotypes with contrasting characteristics (root hairless mutant vs. normal plants; Lynch et al. 2021). This approach helped to disentangle the importance of root hairs in the soil for several plant species, such as barley (Carminati et al. 2017; Gahoonia et al. 2001; Pausch et al. 2016) and *Arabidopsis thaliana* (De Baets et al. 2020). For maize, several root hairless mutants had been described (*rth1–rth6*) and, among them, the *rth3* mutant is particularly useful for this type of study, for being specifically affected in root hair elongation (Hochholdinger et al. 2008; Lynch et al. 2021). This mutant has already been used to understand the role of root hairs in the mobilization of rhizospheric phosphorus (Bilyera et al. 2022) and in controlling the local adaptations of root architecture to soil heterogeneity (Lippold et al. 2021, 2022).

The study of soil aggregation is commonly done by the physical isolation of defined aggregate size classes from the bulk soil. The relative proportions of each size class are then used to gain insight into the processes mediated by the physical arrangement of soil particles, such as the dynamics of SOM formation and degradation (Tisdall and Oades 1982; Six et al. 2004). Most methods that have been used to separate aggregate size fractions are based on wet-sieving approaches to isolate water-stable soil aggregates (Angers et al. 1997; Puget et al. 2000; Bucka et al. 2019). As an alternative method to study the interactions between minerals and microorganisms, the dry-sieving of soil samples after uniaxial crushing has been proposed (Felde et al. 2021). By this method, the samples are first uniaxial crushed to liberate the microaggregates trapped in the macroaggregates and then shaken in a sieve tower to separate samples into the different aggregates size classes (Felde et al. 2021). This aggregate fractionation provides aggregate isolates according to their mechanical stability and, at the same time, avoids potential structural artifacts that can be formed by soil re-wetting, such as the redistribution of C or various other elements between the aggregate fractions (Felde et al. 2021) while at the same time avoiding a change in the microbial community composition that is related to wetting and drying of the sample (Bach et al. 2018).

To gain comprehensive knowledge about the root-induced effects in aggregate stability, it is necessary to use techniques that allow the tracing of the root-derived C. One way to trace the fate of plant root-derived C is the use of $^{13}CO_2$ pulse labeling, tracing of plant photosynthates into rhizodeposition (Kuzyakov and Domanski 2000). The major limitation of this approach is that the ^{13}C enrichment in the bulk soil is usually not high enough to be detected in large pools of C of the plant-soil system, such as the SOM (Studer et al. 2014). In this context, the application of multiple pulses of $^{13}CO_2$ may increase the ^{13}C enrichment of the soil and thus allow the tracking of ^{13}C from the plant and root into different soil C pools. Besides that, the application of a higher number of pulses allows the integration of the fate of the root-C through an extended period of plant growth and development.

The objectives of this study were as follows: (i) to investigate the effects of root hair elongation in the aggregate stability of the rhizosheath; (ii) to evaluate the distribution of recently-deposited root-derived C in rhizosheath aggregates; (iii) to investigate the differences between two $^{13}CO_2$ labeling approaches (single vs. multiple pulse labeling) in the distribution of root-derived C of the aggregate fractions. For such, we compared the stability of rhizosheath aggregates of a *Zea mays* L. root hair defective mutant and a corresponding wild type. In addition, we tracked the fate of root-derived ^{13}C in rhizosheath soil aggregate fractions.

Material and methods

Maize genotypes and soil description

Two maize (*Zea mays* L.) genotypes were used in the study: a root hair defective mutant (*rth3*) and a corresponding wild type (WT). The *rht3* mutant has normal root hair initiation but disturbed elongation (Hochholdinger et al. 2008). The soil used in this study was a Haplic Phaeozem (0–50 cm layer) collected in Schladebach, Germany (51° 18′ 31.41″

N; 12° 6′ 16.31″ E) with the following properties: pH 6.4 (0.01 M $CaCl_2$), total organic carbon (C) 8.5 g kg^{-1}, total nitrogen (N) 0.8 g kg^{-1}, and sand, silt, and clay contents of 33, 48, and 19%, respectively. Additional details about the soil properties are present in Table S1 and described by Vetterlein et al. (2021). The sampled soil was sieved in 4 mm mesh and fertilized to achieve a slightly nutrient-deficient condition for the maize plants (Table S2).

Experimental setup and ^{13}C labeling

The experimental setup followed the recommendations of the interdisciplinary experimental platform for the *Deutsche Forschungsgemeinschaft* (DFG) priority program 2089, "Rhizosphere spatiotemporal organisation— a key to rhizosphere functions" (Vetterlein et al. 2021). In brief, the plants were cultivated in soil columns which consisted of acrylic tubes (25 cm in height, 7 cm inner diameter; Fig. S1) capped in the bottom with a 30 µm nylon mesh screen. The columns were packed with soil up to the first 23 cm height with a density of 1.26 g cm^{-3} (soil mass: 1115 g, soil volume: 885 cm^3) and wrapped in an aluminum foil to prevent algae growth. During the packing, the soil was poured through a horizontally moving 4 mm sieve to avoid particle sorting (Lippold et al. 2021). The maize seeds were surface sterilized with a 10% H_2O_2 solution for 10 min, rinsed with distilled water, and then immersed in a saturated $CaSO_4$ solution (20 mmol L^{-1}) for 3 h to induce germination. Further, the seeds were

sown at 1 cm depth in the soil columns, and a gravel layer was placed on the top to avoid splashing effects due to irrigation. The experimental units were grown in a climate chamber for 21 days under the following conditions: temperature of 22 °C (daytime) and 18 °C (at night); photosynthetic active radiation of 350 µM m^2 s^{-1}; and photoperiod of 12 h. The watering was done on days 1, 5, 7, 11, 14, 17, 19, and 21 after sowing by the application of demineralized water to maintain the volumetric soil water content at 22% (monitored by sample weighing).

Two ^{13}C labeling approaches were evaluated in this study: the application of a single pulse and the application of multiple pulses. The total amount of ^{13}C applied in both labeling approaches was the same, but the frequency at which plants were exposed to the ^{13}C-CO_2 enriched atmosphere was different. The plants were exposed to the ^{13}C-CO_2 enriched atmosphere only one time (on the 21 days after sowing) for single pulse labeling and five times (on the 11, 14, 17, 19, and 21 days after sowing) for multiple pulse labeling (Fig. 1). The total amount of ^{13}C applied was set as 5 g for both treatments. For each pulse, each plant was placed in a labeling chamber (0.82 m^3) and exposed to an artificial ^{13}C-CO_2 enriched atmosphere, which was generated by the reaction of $Na_2^{13}CO_3$ (99% atom%^{13}C) with an acid solution. The plants were randomly placed inside the growing chamber for 4–5 h, and small fans were present in the chamber to proportionate an even distribution of the ^{13}C-CO_2. Each treatment had 4 replicates.
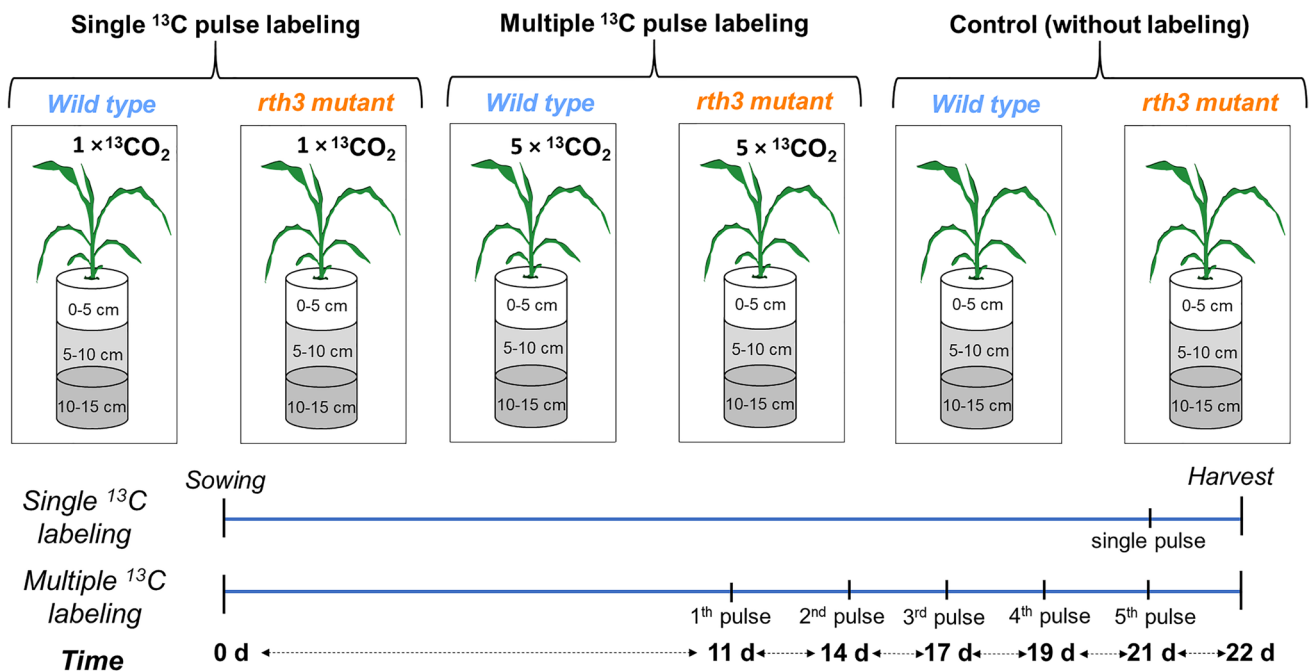
Fig. 1 Schematic representation of the treatments and the time of ^{13}C pulse labeling application in single and multiple pulse labeling approaches

Rhizosheath sampling and aggregate fractionation

After 22 days, the experimental units were harvested, and the soil was carefully pressed out of the columns and separated into three depths: 0–5, 5–10, and 10–15 cm (Fig. 1). The roots and the adhering soil were collected and manually shaken until no more soil became detached. The soil that remained attached to roots after shaking was considered to be the rhizosheath (Brown et al. 2017). The rhizosheath was then separated from the roots by gently brushing. Further, the rhizosheath was air-dried, and the remaining root fragments were picked manually.

The isolation of the aggregate classes was done with the dry-crushing aggregate fractionation method (Felde et al. 2021). This method was chosen instead of the wet-sieving approach because it better preserves the microbial communities, including microscale habitats of the mineral soil matrix, and also avoids redistribution of organic matter and elements between the aggregate size fractions due to soil re-wetting (Felde et al. 2021). The sampled rhizosheath soil was crushed under uniaxial compression in a loading frame (Zwick-Roell, Ulm, Germany) at the constant speed of 250 $\mu m\ min^{-1}$. Subsequently, the crushed samples were sieved in a modified *Casagrande* apparatus, which consisted of two sieves of mesh sizes of 53 and 250 μm and a sieve pan. The tap-sieving frequency was set as 2 Hz and the rhizosheath aggregates were separated into the following fractions: macroaggregates (> 250 μm), larger microaggregates (53–250 μm) and primary small particles and smaller microaggregates (< 53 μm). During this procedure, all the materials (sieves and plates) were carefully cleaned with 99% ethanol between the samples to avoid ^{13}C cross-contamination.

Elemental and isotopic analysis and isotopic calculations

The rhizosheath aggregate size classes of the treatments and the unlabeled references were analyzed for OC, N, and δ^{13}C (‰ V-PDB) in an isotopic ratio mass spectrometer (IRMS delta V Advantage, Thermo Fisher, Dreieich, Germany) coupled with an Elemental Analyzer (Euro EA, Eurovector, Milan, Italy).

Then, the measured δ^{13}C values were converted into ^{13}C atom% and used to calculate the carbon average atomic mass (M_{carbon}—mg $mmol^{-1}$) for each sample with the equation:

$$M_{carbon}(mg\ mmol^{-1}) = (M_{carbon-13} \times {}^{13}C_{atom\%}/100) + (M_{carbon-12} \times (1 - {}^{13}C_{atom\%}/100))$$

where M_{carbon} is the carbon average molar mass of the samples corrected for the ^{13}C enrichment of each sample

(mg $mmol^{-1}$), $M_{carbon-13}$ was considered as 13 mg $mmol^{-1}$, $M_{carbon-12}$ was considered as 12 mg $mmol^{-1}$.

The ^{13}C enrichment in the rhizosheath fractions ($^{13}C_{atom\%\ excess}$) was calculated as the difference between the ^{13}C atom% in the labeled samples ($^{13}C_{atom\%\ labeled}$) and the ^{13}C in the unlabeled references ($^{13}C_{atom\%\ unlabeled}$) with the equation:

$$^{13}C_{atom\%excess}(\%) = {}^{13}C_{atom\%labeled} - {}^{13}C_{atom\%unlabeled}$$

The ^{13}C content (μg of ^{13}C g^{-1}) in the rhizosheath aggregate size classes was calculated with the equation:

$$^{13}C_{content}(\mu g\ g^{-1}) = \frac{^{13}C_{atom\%excess}}{100} \times C_{aggregate} \times \frac{M_{carbon-13}}{M_{carbon}} \times 1000$$

where $^{13}C_{atom\%\ excess}$ is the ^{13}C enrichment in a given aggregate fraction (%); $C_{aggregate}$ is the C content in a given soil aggregate fraction (mg C g^{-1}); $M_{carbon-13}$ was considered as 13 mg $mmol^{-1}$, and M_{carbon} is the average molar mass of the samples corrected for the ^{13}C enrichment (mg C $mmol^{-1}$ C).

The total amount of ^{13}C that was incorporated into the rhizosheath (total ^{13}C recovered) was calculated with the following equation:

$$\text{Total } ^{13}C \text{ recovered}(\mu g) = {}^{13}C_{content} \times mass_{aggregate}$$

where $^{13}C_{content}$ is the ^{13}C content in a given aggregate fraction (μg of ^{13}C g^{-1}); $mass_{aggregate}$ is the total mass of the rhizosheath aggregate.

The distribution of ^{13}C in the aggregate size classes was calculated by the ratio of total ^{13}C recovered in a given fraction and the sum of total ^{13}C recovered in all fractions of a given experimental unit.

Data processing and statistics

The dataset was formed by the elemental and isotopic measurements of each experimental unit (soil column) for each of three depths (0–5, 5–10, 10–15 cm). Since the effects of the genotypes were similar for the different depths, we combined the rhizosheath mass, OC, and N contents of the different depths to present the overall effect of the root hairs in the whole soil column. The original values from each of the depths for the measured variables are presented in Tables S3, S4, and S5, respectively. For the δ^{13}C, values of each layer are presented separately (Table S6).

The differences between the maize genotypes in each of the aggregate fractions was accessed using non-paired t-tests (WT vs. *rth3*). Shapiro–Wilk test was performed to check for normality of the data and homogeneity of variances was checked by Levene's test. All statistical analyses were done in R v. 4.1.2 (R Core Team 2022) with the packages rstatix (Kassambara 2021) and car (Fox and Weisberg

2019), and the graphs were created using the ggplot2 package (Wickham 2016). The probability level to determine significance was $P < 0.05$.

Results

Rhizosheath mass and aggregate distribution

The WT genotype had a rhizosheath mass 2.3 to 2.6 times higher than the *rth3* genotype. The increase in the rhizosheath mass was observed in all aggregate size classes, regardless of the labeling approach (Table 1). Overall, macroaggregates comprised the majority portion of rhizospheric soil mass (56% ± 3), followed by the large microaggregates (37% ± 3) and smaller microaggregates (8% ± 4; Table 2).

Organic carbon and nitrogen content and their distribution in the aggregates

No differences between the genotypes were observed in the organic carbon (OC) and nitrogen (N) content of the aggregate fractions, except for the 53–250 μm fraction in the single pulse labeling approach (Table 1). In this fraction, the WT genotype had a 5% higher OC content and a 4% higher N content in comparison with the *rth3* mutant. Nevertheless, this was not observed in the multiple pulse labeling, which showed no significant difference between the genotypes (Table 1). Among the aggregate fractions, macroaggregates (> 250 μm) exhibited the smallest contents of OC and N (8.5 and 0.9 mg g^{-1}, respectively; Table 1). Meanwhile the microaggregate fractions (250–53 μm and < 53 μm) had the highest OC and N contents (10.4 mg g^{-1} and 1.1 mg g^{-1}, respectively; Table 1). The C:N ratio was not affected by the genotypes and was similar in all aggregate size classes (mean of 9.6; Table 1).

Overall, OC distribution showed the same distribution pattern as the rhizosheath mass and was not affected by

Table 1 Rhizosheath soil mass, organic carbon (OC) content (mg g^{-1} fraction), nitrogen content (mg g^{-1} fraction), and carbon-to-nitrogen ratio (C:N ratio) in aggregate fractions (> 250 μm, 53–250 μm, and < 53 μm) for single and multiple ^{13}C pulse labeling treatments and maize genotypes (wild type and *rth3* mutant). Means (± SD) of maize genotypes followed by different lowercase letters are different (*p* < 0.05)

Variable	^{13}C pulse labeling	Aggregate fractions						Combined fractions[1]	
		> 250 μm		53–250 μm		< 53 μm			
		WT	*rth3*	WT	*rth3*	WT	*rth3*	WT	*rth3*
Rhizosheath mass (g)	Single	6.8 ± 2.5 a	3.0 ± 1.2 b	4.1 ± 1.0 a	2.0 ± 0.8 b	1.5 ± 1.4	0.4 ± 0.2	12.4 ± 2.2 a	5.3 ± 1.5 b
	Multiple	6.4 ± 1.7 a	2.4 ± 0.8 b	4.0 ± 0.5 a	1.5 ± 0.4 b	0.8 ± 0.1 a	0.3 ± 0.1 b	11.2 ± 1.4 a	4.2 ± 0.7 b
OC content (mg g^{-1} fraction)	Single	8.6 ± 0.2	8.3 ± 0.3	10.6 ± 0.1 a	10.0 ± 0.2 b	10.9 ± 0.2	10.5 ± 0.4	10.0 ± 0.3	9.6 ± 0.3
	Multiple	8.3 ± 0.5	8.6 ± 0.2	10.2 ± 0.2	10.0 ± 0.1	10.6 ± 0.4	10.7 ± 0.1	9.7 ± 0.4	9.8 ± 0.3
N content (mg g^{-1} fraction)	Single	0.9 ± 0.3	0.9 ± 0.2	1.1 ± 0.2 a	1.0 ± 0.2 b	1.1 ± 0.1	1.1 ± 0.1	1.0 ± 0.1	1.0 ± 0.1
	Multiple	0.9 ± 0.4	0.9 ± 0.4	1.1 ± 0.2	1.0 ± 0.1	1.1 ± 0.1	1.1 ± 0.1	1.0 ± 0.1	1.0 ± 0.1
C:N ratio	Single	9.6 ± 0.1	9.6 ± 0.2	9.8 ± 0.1	9.6 ± 0.1	9.7 ± 0.2	9.7 ± 0.1	9.7 ± 0.2	9.7 ± 0.1
	Multiple	9.5 ± 0.1	9.4 ± 0.3	9.8 ± 0.1	9.6 ± 0.1	9.7 ± 0.1	9.7 ± 0.2	9.7 ± 0.1	9.6 ± 0.2

[1]Rhizosheath mass of the combined fractions was calculated from the sum of the different aggregate fractions

Table 2 Rhizosheath soil mass and organic carbon (OC) distribution in the aggregate fractions (> 250 μm, 53–250 μm, and < 53 μm) for single and multiple pulse labeling treatments and maize genotypes (wild type and *rth3* mutant). Means (± SD) are presented

Variable	^{13}C pulse labeling	Aggregate fractions					
		> 250 μm		53–250 μm		< 53 μm	
		WT	*rth3*	WT	*rth3*	WT	*rth3*
Rhizosheath mass distribution (%)	Single	54 ± 2	56 ± 6	35 ± 8	37 ± 4	11 ± 7	6 ± 2
	Multiple	67 ± 8	57 ± 2	36 ± 3	36 ± 2	7 ± 2	7 ± 1
OC distribution (%)	Single	49 ± 2	52 ± 6	39 ± 9	41 ± 4	13 ± 8	7 ± 2
	Multiple	51 ± 4	53 ± 1	40 ± 3	39 ± 1	8 ± 1	8 ± 1

the root hair elongation (Table 2). The macroaggregates (> 250 μm) comprised the majority portion of rhizosheath OC (51%), while larger microaggregates (53–250 μm) and smaller microaggregates (< 53 μm) accounted for 40% and 9% of the soil OC, respectively (Table 2).

^{13}C tracing in the rhizosheath aggregates

Root hair elongation did not affect the ^{13}C enrichment (δ^{13}C) in any of the rhizosheath aggregate size classes (Table S6 and Fig. 2). The only exception was the < 53 μm fraction of the 5–10 cm layer in the multiple pulse labeling approach (Table S6). In this fraction, the WT genotype had a higher δ^{13}C value (− 5.0‰) in comparison to the root hair defective mutant (− 17.4‰). Nevertheless, this was not observed in the single pulse labeling approach, which showed no significant difference between the genotypes (Table S6). Overall, the multiple ^{13}C pulse labeling approach yielded a higher ^{13}C enrichment in all aggregate fractions in comparison with the single pulse approach, and both labeling approaches were significantly more enriched in ^{13}C than the unlabeled control (mean of − 26.1‰; Table S7).

We observed that the total ^{13}C recovered in the rhizosheath differed among the labeling approaches. For the single pulse labeling, no differences between the maize genotypes were observed in any of the aggregate size classes (Fig. 3). Meanwhile, in the multiple pulse labeling, the total ^{13}C amount recovered in rhizosheath for the WT genotype was 3.4 times higher than for the *rth3* mutant and significant differences between the genotypes were observed in the > 250 μm and 53–250 μm fractions (Fig. 3).

Despite these differences, the distribution of ^{13}C within the aggregate size classes was not affected by the maize genotypes and followed the same trend observed for the aggregate mass and OC distribution (Fig. 4). The majority of the ^{13}C was found in the macroaggregate fractions (57%), followed by the larger microaggregates (38%) and smaller microaggregates (5%).

Discussion

Root hair elongation provides an extended rhizosheath but does not affect the aggregate size distribution

We found that the rhizosheath mass of the maize genotype with normal root hairs was 2.5 times larger in relation to the maize genotype with defective root hair elongation (Table 1). This confirms the increase in root-affected soil volumes due to the extension via root hair elongation, as found in previous studies (Watt et al. 1994; McCully 1999; Haling et al. 2014; Koebernick et al. 2017; Burak et al. 2021). The mechanism of rhizosheath formation is described as a combination of two root-driven processes: (i) the physical enmeshment of soil particles by root hairs and the associated hyphosphere, and (ii) the binding of mineral particles resulting from the gluing action of rhizodeposits and the microbial byproducts from their processing (Ritz and Young 2004; Gould et al. 2016; Totsche et al. 2018; Vidal et al. 2018; Burak et al. 2021; Xu et al. 2022). In the mutant with defective root hair elongation, the rhizosheath aggregation relies only on the chemical

Fig. 2 ^{13}C excess content (μg ^{13}C g^{-1} fraction) in the rhizosheath (total) and in the aggregates size classes (> 250 μm, 53–250 μm, and < 53 μm) for single and multiple pulse labeling treatments and maize genotypes (wild type and *rth3* mutant). Asterisks denote statistically significant differences at 5% between the wild type and *rth3* mutant for a given fraction
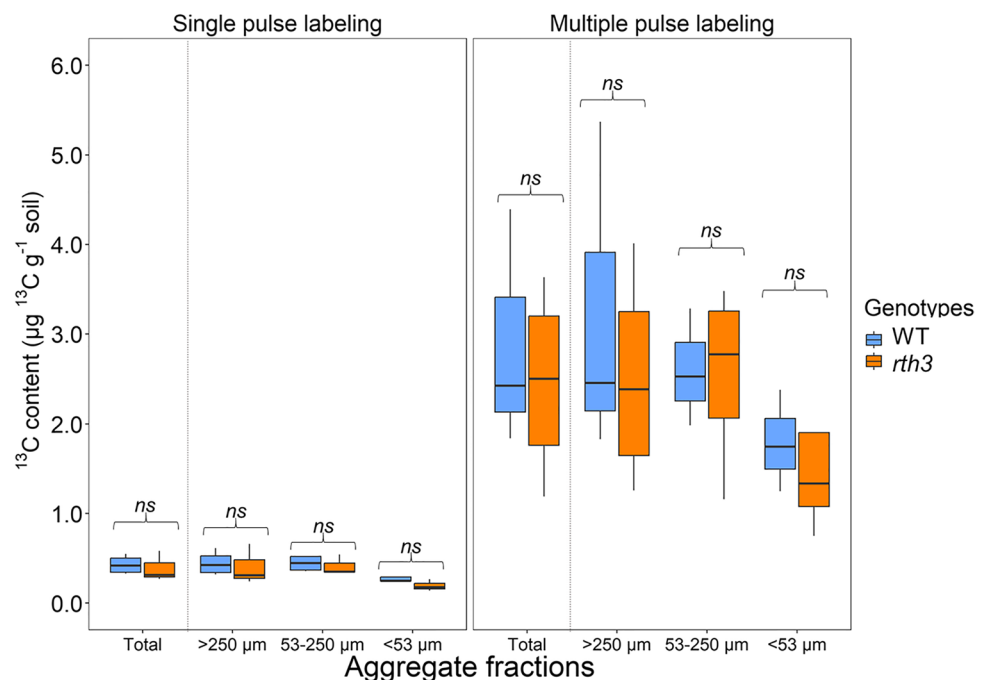
Fig. 3 Total amount of excess ^{13}C (µg ^{13}C) recovered in the whole rhizosheath (total) and the aggregates size classes (> 250 µm, 53–250 µm, and < 53 µm) for single and multiple pulse labeling treatments and maize genotypes (wild type and *rth3* mutant). Asterisks denote statistically significant differences at 5% between the wild type and *rth3* mutant for a given fraction
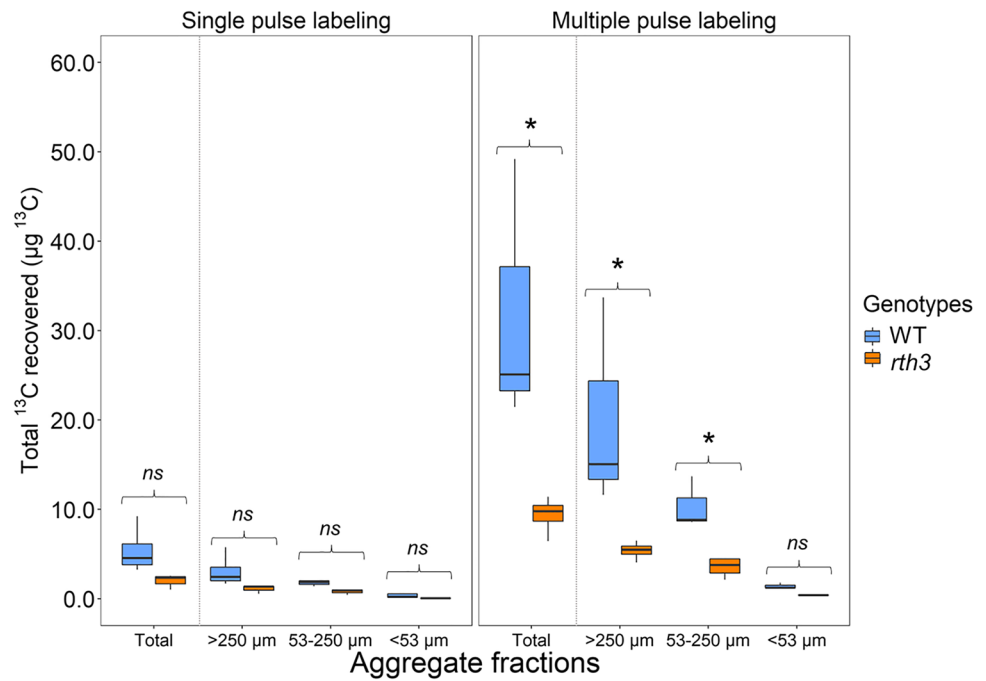
Fig. 4 Distribution of ^{13}C (%— µg ^{13}C fraction µg^{-1} ^{13}C soil) in the aggregate size classes (> 250 µm, 53–250 µm, and < 53 µm) for single and multiple pulse labeling treatments and maize genotypes (wild type and *rth3* mutant). Lowercase letters denote statistically significant differences at 5% between the wild type and *rth3* mutant for a given fraction
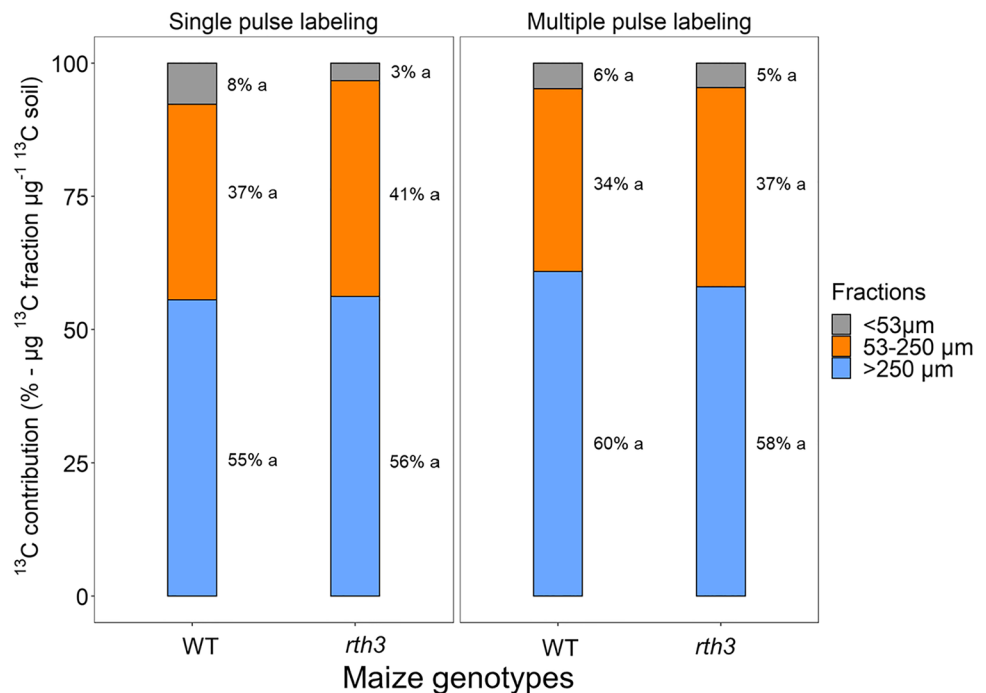
binding of soil particles resulting from root exudation and mucilage production (Naveed et al. 2018). Since root exudates have a very limited diffusion in the soil mainly because they are rapidly consumed by microorganisms, the extent of the soil volume this mechanism can act on is spatially limited (Kuzyakov et al. 2003). In this context, only soil particles that are in closer vicinity to the root are bound as rhizosheath,

which explains the limited rhizosheath development in the genotypes with defective root hair elongation.

On the other hand, in the WT genotype, the enhanced rhizosheath mass went along with a higher amount of root-derived ^{13}C recovered in the rhizosheath aggregates (Fig. 3). This result suggests that root hair elongation leads not only to the physical entanglement of the soil aggregates, but also to an increase in the root exudates' diffusion towards the

soil. The enhancement of the root C in rhizosheath due to root hairs presence has been reported by Holz et al. (2018), who observed that the amount of ^{14}C in the rhizosheath was 8 times higher in a barley genotype with normal root hairs in comparison to a mutant without root hairs. Root hairs were shown to influence the connectivity of pores around the root (Koebernick et al. 2017), and this mechanism may be responsible for promoting the transference of C through the extended rhizosheath.

An extended rhizosheath is highly beneficial for the rhizosphere microbiome (Sasse et al. 2018) and hence also for the conversion of root C inputs into slow-cycling SOM pools, such as the mineral-associated OM in the different aggregate size classes. The region affected by root is spatially constrained up to a few millimeters towards the roots, and evidence from the literature suggests this factor can limit the amount of C that can be incorporated into mineral-associated OM (Kuzyakov and Cheng 2001; Sokol and Bradford 2019). An enhanced rhizosheath provided by root hairs allows a higher interaction of root C inputs with soil mineral surfaces that are responsible for the C long-term persistence in the soils (Holz et al. 2018; Sokol and Bradford 2019). This rhizosphere extension can additionally be fostered by mycorrhization and, thus an extended hyphosphere (Vidal et al. 2018).

To our surprise, the extended rhizosheath in the WT genotype was not accompanied by an increase in the proportion of macroaggregates, and both maize genotypes showed a similar aggregate size distribution in the rhizosheath (Fig. 4). As summarized by Poirier et al. (2018), it is often considered that root hairs specifically have a role in the formation of macroaggregates. In contrast, we show that the contribution of root hairs is to extend the soil volume that is entangled and receives rhizodeposition, which in turn induces aggregate formation. Nevertheless, since the enrichment of the non-rhizosheath soil (bulk soil) was not evaluated in our study, our conclusion are limited only to the rhizosheath and it is not possible to affirm about the diffusion of ^{13}C beyond this region. Despite of this limitation, our data confirm that root hairs increase the size of the rhizosheath, and at the same time, we provide evidence that the mechanisms that lead to the formation of soil aggregates—as delineated from the aggregate size distribution—are not affected.

Flow of C in the rhizosheath: from macroaggregates to microaggregates

Based on the fate of the root-derived ^{13}C, we demonstrated that the majority of the recently deposited root C was recovered in the macroaggregate fraction (57%), regardless of the genotype or labeling approach (single vs. multiple pulse labeling; Fig. 4). This highlights the role of macroaggregates as preferential soil structures fostering the allocation of new SOM (Skjemstad et al. 1990; Angers and Giroux 1996; Angers et al. 1997; Puget et al. 2000; Witzgall et al. 2021). According to the aggregate hierarchy theory, macroaggregates are stabilized by transient and relatively undecomposed organic binding agents, which can include rhizodeposits and other organic compounds that act as a nuclei for the formation of macroaggregates (Oades and Waters 1991; Baumert et al. 2018; Witzgall et al. 2021).

Despite the clear differences in the amount of the recovered root-derived C in the analyzed rhizosheath aggregates, our results show that both genotypes had a similar ^{13}C distribution in the rhizosheath (Fig. 4). This finding demonstrates that the allocation of initial root-derived C into different aggregate size classes in the rhizosheath is controlled by intrinsic soil properties rather than root hair elongation. We show that macroaggregates account for the majority of OC found in the soil, despite having the smallest OC content (Tables 1 and 2). The smaller content of OC found in the macroaggregates can be explained by the inclusion of sand-sized particles (quartz particles) in this fraction, which dilutes its OC content in relation to the other fractions (Felde et al. 2021). Although sand-sized particles are regarded as not an aggregation binding agent (Six et al. 2000), the way of separating aggregates via sieving yields this mixture of aggregates and primary particles (Bucka et al. 2019; Felde et al. 2021).

Multiple pulse labeling allowed a better separation of the aggregate size classes in the rhizosheath

Our results show that the multiple pulse labeling leads to a higher ^{13}C enrichment in all rhizosheath aggregate size fractions in relation to the single pulse labeling (Fig. 3). Nevertheless, the distribution of ^{13}C among the different aggregate size classes was very similar in both labeling approaches (Fig. 4). Regardless of this, some limitations of our experimental approach needs to be considered for the interpretation of the results. First, rhizodeposition is a process that is heavily influenced by spatial and temporal variations of C assimilation and partition (Studer et al. 2014; Wei et al. 2021). In this context, even diurnal patterns can modify the assimilation of the ^{13}C and, consequently, its transference to the soil and to the rhizosphere microbiota (Baraniya et al. 2018). Interestingly, irrespective of the temporal of alterations, the allocation pattern of both approaches led to similar distributions in the rhizosheath aggregates, which suggests that the mechanisms leading to the sequestration of initially root-derived C into distinct soil aggregates were not affected by the labeling approach. Second, in our study, the

artificial input of ^{13}C-CO$_2$ in the labeling chamber increased the levels of CO$_2$ beyond the levels commonly found in the atmosphere. It is known that the enhancement of CO$_2$ can affect the photosynthetic rate of the plants and, concomitantly, the rhizodeposition and the allocation of ^{13}C in the soil–plant system (Wang et al. 2015). Regardless of these factors, our results suggest that the multiple pulse labeling approach allowed a better resolution in terms of detectability of the ^{13}C signal in minor aggregate size fractions to separate the treatment effects on the rhizosheath structure and SOM formation.

Conclusions

We investigated the role of root hair elongation in rhizosheath aggregate formation and the allocation of root-derived C into its aggregate size fractions. We cultivated two distinct maize genotypes with contrasting root hair elongation for 22 days under controlled environmental conditions and used ^{13}C pulse labeling to track the distribution of recently-deposited root C in rhizosheath aggregates. Under the conditions of the study, we observed that root hair elongation enhanced the rhizosheath mass and the total amount of root-derived C therein. However, this effect was not followed by a change in the aggregate size distribution, suggesting that the aggregate formation in the rhizosheath is controlled by intrinsic soil properties rather than root hair action.

Moreover, we also show that the majority of root-derived ^{13}C in the rhizosheath was allocated in the macroaggregates (57%), whereas overall, the distribution of the C allocation into specific aggregate size classes was not affected by root hair elongation. Both single and multiple pulse labeling approaches had proportionated similar results for the ^{13}C distribution in the rhizosheath, but multiple pulse labeling allowed the separation of differences between the genotypes in the aggregate size classes.

Declarations

References

Albalasmeh AA, Ghezzehei TA (2014) Interplay between soil drying and root exudation in rhizosheath development. Plant Soil 374:739–751. https://doi.org/10.1007/s11104-013-1910-y

Angers DA, Giroux M (1996) Recently deposited organic matter in soil water-stable aggregates. Soil Sci Soc Am J 60:1547–1551. https://doi.org/10.2136/sssaj1996.03615995006000050037x

Angers DA, Recous S, Aita C (1997) Fate of carbon and nitrogen in water-stable aggregates during decomposition of ^{13}C^{15}N-labelled wheat straw *in situ*. Eur J Soil Sci 48:295–300. https://doi.org/10.1111/j.1365-2389.1997.tb00549.x

Bach EM, Williams RJ, Hargreaves SK, Yang F, Hofmockel KS (2018) Greatest soil microbial diversity found in micro-habitats. Soil Biol 118:217–226. https://doi.org/10.1016/j.soilbio.2017.12.018

Baraniya D, Nannipieri P, Kublik S, Vestergaard G, Schloter M, Schöler A (2018) The impact of the diurnal cycle on the microbial transcriptome in the rhizosphere of barley. Microb Ecol 75:830–833. https://doi.org/10.1007/s00248-017-1101-0

Bardgett RD, Mommer L, De Vries FT (2014) Going underground: root traits as drivers of ecosystem processes. Trends Ecol Evol 29:692–699. https://doi.org/10.1016/j.tree.2014.10.006

Baumert VL, Vasilyeva NA, Vladimirov AA, Meier IC, Kögel-Knabner I, Müller CW (2018) Root exudates induce soil macroaggregation facilitated by fungi in subsoil. Front Environ Sci 6:140. https://doi.org/10.3389/fenvs.2018.00140

Baumert VL, Forstner SJ, Zethof JHT, Vogel C, Heitkötter J, Schulz S, Kögel-Knabner I, Müller CW (2021) Root-induced fungal growth triggers macroaggregation in forest subsoils. Soil Biol Biochem 157:108244. https://doi.org/10.1016/j.soilbio.2021.108244

Bengough AG, Loades K, McKenzie BM (2016) Root hairs aid soil penetration by anchoring the root surface to pore walls. J Exp Bot 67:1071–1078. https://doi.org/10.1093/jxb/erv560

Bilyera N, Hummel C, Daudin G, Santangeli M, Zhang X, Santner J, Lippold E, Schlüter S, Bertrand I, Wenzel W, Spielvogel S, Vetterlein D, Razavi BS, Oburger E (2022) Co-localised phosphorus mobilization processes in the rhizosphere of field-grown maize jointly contribute to plant nutrition. Soil Biol Biochem 165:108497. https://doi.org/10.1016/j.soilbio.2021.108497

Brown LK, George TS, Neugebauer K, White PJ (2017) The rhizosheath – a potential trait for future agricultural sustainability occurs in orders throughout the angiosperms. Plant Soil 418:115–128. https://doi.org/10.1007/s11104-017-3220-2

Bucka FB, Kölbl A, Uteau D, Peth S, Kögel-Knabner I (2019) Organic matter input determines structure development and aggregate

formation in artificial soils. Geoderma 354:113881. https://doi.org/10.1016/j.geoderma.2019.113881

Bucka FB, Felde VJMNL, Peth S, Kögel-Knabner I (2021) Disentangling the effects of OM quality and soil texture on microbially mediated structure formation in artificial model soils. Geoderma 403:115213. https://doi.org/10.1016/j.geoderma.2021.115213

Burak E, Quinton JN, Dodd IC (2021) Root hairs are the most important root trait for rhizosheath formation of barley (*Hordeum vulgare*), maize (*Zea mays*) and *Lotus japonicus* (*Gifu*). Ann Bot 128:45–57. https://doi.org/10.1093/aob/mcab029

Carminati A, Passioura JB, Zarebanadkouki M, Ahmed MA, Ryan PR, Watt M, Delhaize E (2017) Root hairs enable high transpiration rates in drying soils. New Phytol 216:771–781. https://doi.org/10.1111/nph.14715

De Baets S, Denbigh TDG, Smyth KM, Eldridge BM, Weldon L, Higgins B, Matyjaszkiewicz A, Meersmans J, Larson ER, Chenchiah IV, Liverpool TB, Quine TA, Grierson CS (2020) Micro-scale interactions between Arabidopsis root hairs and soil particles influence soil erosion. Commun Biol 3:164. https://doi.org/10.1038/s42003-020-0886-4

De León-González F, Gutiérrez-Castorena MC, González-Chávez MCA, Castillo-Juárez H (2007) Root-aggregation in a pumiceous sandy soil. Geoderma 142:308–317. https://doi.org/10.1016/j.geoderma.2007.08.023

Dolan L, Costa S (2001) Evolution and genetics of root hair stripes in the root epidermis. J Exp Bot 52:413–417. https://doi.org/10.1093/jxb/52.suppl_1.413

Felde VJMNL, Schweizer SA, Biesgen D, Ulbrich A, Uteau D, Knief C, Graf-Rosenfellner M, Kögel-Knabner I, Peth S (2021) Wet sieving versus dry crushing: Soil microaggregates reveal different physical structure, bacterial diversity and organic matter composition in a clay gradient. Eur J Soil Sci 72:810–828. https://doi.org/10.1111/ejss.13014

Fox J, Weisberg S (2019) An R Companion to Applied Regression

Gahoonia TS, Nielsen NE, Joshi PA, Jahoor A (2001) A root hairless barley mutant for elucidating genetic of root hairs and phosphorus uptake. Plant Soil 235:211–219. https://doi.org/10.1023/A:1011993322286

Gould IJ, Quinton JN, Weigelt A, De Deyn GB, Bardgett RD (2016) Plant diversity and root traits benefit physical properties key to soil function in grasslands. Ecol Lett 19:1140–1149. https://doi.org/10.1111/ele.12652

Haling RE, Brown LK, Bengough AG, Valentine TA, White PJ, Young IM, George TS (2014) Root hair length and rhizosheath mass depend on soil porosity, strength and water content in barley genotypes. Planta 239:643–651. https://doi.org/10.1007/s00425-013-2002-1

Hochholdinger F, Wen T-J, Zimmermann R, Chimot-Marolle P, Da Costa e Silva O, Bruce W, Lamkey KR, Wienand U, Schnable PS (2008) The maize (*Zea mays L.*) roothairless3 gene encodes a putative GPI-anchored, monocot-specific, COBRA-like protein that significantly affects grain yield. Plant J 54:888–898. https://doi.org/10.1111/j.1365-313X.2008.03459.x

Holz M, Zarebanadkouki M, Kuzyakov Y, Pausch J, Carminati A (2018) Root hairs increase rhizosphere extension and carbon input to soil. Ann Bot 121:61–69. https://doi.org/10.1093/aob/mcx127

Jungk A (2001) Root hairs and the acquisition of plant nutrients from soil. J Soil Sci Plant Nutr 164:121–129. https://doi.org/10.1002/1522-2624(200104)164:2%3c121::AID-JPLN121%3e3.0.CO;2-6

Kassambara A (2021) rstatix: pipe-friendly framework for basic statistical tests

Koebernick N, Daly KR, Keyes SD, George TS, Brown LK, Raffan A, Cooper LJ, Naveed M, Bengough AG, Sinclair I, Hallett PD, Roose T (2017) High-resolution synchrotron imaging shows that root hairs influence rhizosphere soil structure formation. New Phytol 216:124–135. https://doi.org/10.1111/nph.14705

Kuzyakov Y, Razavi BS (2019) Rhizosphere size and shape: temporal dynamics and spatial stationarity. Soil Biol Biochem 135:343–360. https://doi.org/10.1016/j.soilbio.2019.05.011

Kuzyakov Y, Domanski G (2000) Carbon input by plants into the soil. Review J Soil Sci Plant Nutr 163:421–431. https://doi.org/10.1002/1522-2624(200008)163:4%3c421::AID-JPLN421%3e3.0.CO;2-R

Kuzyakov Y, Cheng W (2001) Photosynthesis controls of rhizosphere respiration and organic matter decomposition. Soil Biol Biochem 33:1915–1925. https://doi.org/10.1016/S0038-0717(01)00117-1

Kuzyakov Y, Raskatov A, Kaupenjohann M (2003) Turnover and distribution of root exudates of *Zea mays*. Plant Soil 254(317):327. https://doi.org/10.1023/A:1025515708093

Lippold E, Phalempin M, Schlüter S, Vetterlein D (2021) Does the lack of root hairs alter root system architecture of Zea mays? Plant Soil 467:267–286. https://doi.org/10.1007/s11104-021-05084-8

Lippold E, Lucas M, Fahrenkampf T, Schlüter S, Vetterlein D (2022) Macroaggregates of loam in sandy soil show little influence on maize growth, due to local adaptations of root architecture to soil heterogeneity. Plant Soil 478:163–175. https://doi.org/10.1007/s11104-022-05413-5

Lynch JP, Strock CF, Schneider HM, Sidhu JS, Ajmera I, Galindo-Castañeda T, Klein SP, Hanlon MT (2021) Root anatomy and soil resource capture. Plant Soil 466:21–63. https://doi.org/10.1007/s11104-021-05010-y

McCully ME (1999) Roots in soil: unearthing the complexities of roots and their rhizospheres. Annu Rev Plant Physiol Plant Mol Biol 50:695–718. https://doi.org/10.1146/annurev.arplant.50.1.695

Naveed M, Brown LK, Raffan AC, George TS, Bengough AG, Roose T, Sinclair I, Koebernick N, Cooper L, Hallett PD (2018) Rhizosphere-scale quantification of hydraulic and mechanical properties of soil impacted by root and seed exudates. Vadose Zone J 17:170083. https://doi.org/10.2136/vzj2017.04.0083

Oades J, Waters A (1991) Aggregate Hierarchy in soils. Soil Res 29:815. https://doi.org/10.1071/SR9910815

Pausch J, Loeppmann S, Kühnel A, Forbush K, Kuzyakov Y, Cheng W (2016) Rhizosphere priming of barley with and without root hairs. Soil Biol Biochem 100:74–82. https://doi.org/10.1016/j.soilbio.2016.05.009

Poirier V, Roumet C, Munson AD (2018) The root of the matter: Linking root traits and soil organic matter stabilization processes. Soil Biol Biochem 120:246–259. https://doi.org/10.1016/j.soilbio.2018.02.016

Puget P, Chenu C, Balesdent J (2000) Dynamics of soil organic matter associated with particle-size fractions of water-stable aggregates: dynamics of soil organic matter in water-stable aggregates. Eur J Soil Sci 51:595–605. https://doi.org/10.1111/j.1365-2389.2000.00353.x

R Core Team (2022) R: a language and environment for statistical computing. R Foundation for Statistical Computing

Ritz K, Young IM (2004) Interactions between soil structure and fungi. Mycologist 18:52–59. https://doi.org/10.1017/S0269915X04002010

Sasse J, Martinoia E, Northen T (2018) Feed your friends: do plant exudates shape the root microbiome? Trends Plant Sci 23:25–41. https://doi.org/10.1016/j.tplants.2017.09.003

Six J, Elliott ET, Paustian K (2000) Soil macroaggregate turnover and microaggregate formation: a mechanism for C sequestration under no-tillage agriculture. Soil Biol Biochem 32:2099–2103. https://doi.org/10.1016/S0038-0717(00)00179-6

Six J, Bossuyt H, Degryze S, Denef K (2004) A history of research on the link between (micro)aggregates, soil biota, and soil organic matter dynamics. Soil Tillage Res 79:7–31. https://doi.org/10.1016/j.still.2004.03.008

Skjemstad J, Lefeuvre R, Prebble R (1990) Turnover of soil organic matter under pasture as determined by ^{13}C natural abundance. Soil Res 28:267. https://doi.org/10.1071/SR9900267

Sokol NW, Bradford MA (2019) Microbial formation of stable soil carbon is more efficient from belowground than aboveground input. Nat Geosci 12:46–53. https://doi.org/10.1038/s41561-018-0258-6

Studer MS, Siegwolf RTW, Abiven S (2014) Carbon transfer, partitioning and residence time in the plant-soil system: a comparison of two $^{13}CO_2$ labelling techniques. Biogeosciences 11:1637–1648. https://doi.org/10.5194/bg-11-1637-2014

Tisdall JM, Oades JM (1982) Organic matter and water-stable aggregates in soils. J Soil Sci 33:141–163. https://doi.org/10.1111/j.1365-2389.1982.tb01755.x

Totsche KU, Amelung W, Gerzabek MH, Guggenberger G, Klumpp E, Knief C, Lehndorff E, Mikutta R, Peth S, Prechtel A, Ray N, Kögel-Knabner I (2018) Microaggregates in soils. J Soil Sci Plant Nutr 181:104–136. https://doi.org/10.1002/jpln.201600451

Vetterlein D, Lippold E, Schreiter S, Phalempin M, Fahrenkampf T, Hochholdinger F, Marcon C, Tarkka M, Oburger E, Ahmed M, Javaux M, Schlüter S (2021) Experimental platforms for the investigation of spatiotemporal patterns in the rhizosphere—Laboratory and field scale. J Soil Sci Plant Nutr 184:35–50. https://doi.org/10.1002/jpln.202000079

Vidal A, Hirte J, Bender SF, Mayer J, Gattinger A, Höschen C, Schädler S, Iqbal TM, Mueller CW (2018) Linking 3D soil structure and plant-microbe-soil carbon transfer in the rhizosphere. Front Environ Sci Science 6:9. https://doi.org/10.3389/fenvs.2018.00009

Wang M, Xie B, Fu Y, Dong C, Hui L, Guanghui L, Liu H (2015) Effects of different elevated CO_2 concentrations on chlorophyll contents, gas exchange, water use efficiency, and PSII activity on C3 and C4 cereal crops in a closed artificial ecosystem. Photosynth Res 126:351–362. https://doi.org/10.1007/s11120-015-0134-9

Watt M, McCully ME, Jeffree CE (1993) Plant and bacterial mucilages of the maize rhizosphere: Comparison of their soil binding properties and histochemistry in a model system. Plant Soil 151:151–165. https://doi.org/10.1007/BF00016280

Watt M, McCully ME, Canny MJ (1994) Formation and stabilization of rhizosheaths of *Zea mays* L. (effect of soil water content). Plant Physiol 106:179–186. https://doi.org/10.1104/pp.106.1.179

Wei S, Jacquiod S, Philippot L, Blouin M, Sørensen SJ (2021) Spatial analysis of the root system coupled to microbial community inoculation shed light on rhizosphere bacterial community assembly. Biol Fertil Soils 57:973–989. https://doi.org/10.1007/s00374-021-01590-0

Wickham H (2016) ggplot2: elegant graphics for data analysis

Witzgall K, Vidal A, Schubert DI, Höschen C, Schweizer SA, Buegger F, Pouteau V, Chenu C, Mueller CW (2021) Particulate organic matter as a functional soil component for persistent soil organic carbon. Nat Commun 12:4115. https://doi.org/10.1038/s41467-021-24192-8

Xu Y, Gao X, Pei J, Sun L, Wang J (2022) Crop root vs. shoot incorporation drives microbial residue carbon accumulation in soil aggregate fractions. Biol Fertil Soils 58:843–854. https://doi.org/10.1007/s00374-022-01666-5